# Absorption and Fluorescence Spectroscopic Studies of the $Ca^{2+}$-Dependent Lipid Binding Protein p36: The Annexin Repeat as the $Ca^{2+}$ Binding Site†

Gerard Marriott,*,‡,§ William R. Kirk,*,‡ Nils Johnsson,‖ and Klaus Weber‖
*Departments of Molecular Biology and Biochemistry, Max Planck Institute for Biophysical Chemistry, D-3400 Goettingen, FRG*

*Received December 21, 1989; Revised Manuscript Received April 5, 1990*

ABSTRACT: The existence of a single tryptophan residue in the protein p36, a member of a recently characterized family of $Ca^{2+}$ binding proteins called annexins, is exploited to provide unique spectroscopic information on the annexin repeat motif and its role in $Ca^{2+}$ binding. The differences in ultraviolet absorption and fluorescence excitation upon $Ca^{2+}$ binding are interpreted solely in terms of this tryptophan, which, in view of the pronounced blue-shifts and the presence of vibronic structure, seems to reside in a highly nonpolar environment. The fluorescence emission from the protein is correspondingly blue-shifted, and it is found to transfer energy in resonance with $Tb^{3+}$ absorption lines in the near-ultraviolet. This effect allows us to locate the $Tb^{3+}$ and, by implication, the $Ca^{2+}$ binding site to within ca. 8 Å of the tryptophan residue.

The recently defined protein family of $Ca^{2+}$ binding proteins (annexins) is based on a common structural principle. A short protease-sensitive N-terminal tail domain, highly divergent in length and sequence, protrudes from a core domain built from homologous segments of approximately 75 residues, each 4- or 8-fold tandemly repeated [for review, see Klee (1988)]. The core domain displays the $Ca^{2+}$ and lipid binding properties while the tails seem to have a regulatory function and harbor established phosphorylation sites (Glenney, 1986; Johnsson et al., 1986a,b). Although the precise function of the annexins has not been firmly established, they are thought to be involved in membrane phenomena including exocytosis. Intestinal epithelial cells are a rich source for two of the annexins. The first, protein II, is a monomer of apparent molecular weight of 32 000, while the second, p36, is a substrate of the tyrosine-specific protein kinase $pp60^{src}$ and is isolated as a heterotetrameric complex with a unique peptide ligand, p11 (Gerke & Weber, 1984). The p11 binding site covers the N-acetylated terminal 12 residues of p36, which can adopt an amphipathic helical structure either in the p36–p11 complex or as free peptide once trifluoroethanol is added to 50% (Johnsson et al., 1988).

The ultraviolet absorption and fluorescence emission of tryptophan residues in proteins are often used to investigate relationships between protein structure, function, and dynamics (Xu & Weber, 1982; Beechem & Brand, 1986; Demchenko, 1986). Recently, these techniques have also been applied in this laboratory (Shadle et al., 1985; Johnsson et al., 1988) to investigate the association interactions between p36 or p36-derived peptides derivatized with an extrinsic fluorophore and p11 (Johnsson et al., 1988). The wealth of information obtained prompted us to extend these investigations into the effects of added $Ca^{2+}$ on the absorption and intrinsic fluorescence of p36 and p36–p11 complex as well as protein II as obtained from a variety of vertebrate sources by use of steady-state and time-resolved fluorescence spectroscopic techniques. Such information can be used to probe the molecular environment surrounding the intrinsic fluorophore (Scarlata et al., 1984; Beechem & Brand, 1986; Demchenko, 1986). The detailed spectroscopic information obtained in this way is of limited use unless the protein possesses a single tryptophan (Strickland et al., 1972; Longworth, 1983). This rather stringent requirement is fulfilled by p36 and protein II. They both possess a single tryptophan residue located in the third homology segment of the core (Johnsson et al., 1986a; Weber et al., 1987). Interestingly, the relative position of the tryptophan residue is shifted by seven positions toward the N-terminus when protein II and p36 are aligned (Saris et al., 1986; Weber et al., 1987). An additional advantage of the system of annexins lies in the fact that the tryptophan content of the heterotetrameric p36–p11 complex lies entirely in the p36 subunit; this situation provides us with the opportunity to observe the differential effects of $Ca^{2+}$ binding upon the isolated proteins vs the complete tetramer by use of the identical fluorescence "marker". On the basis of the spectroscopic data described in this study, we present our preliminary conclusions on the nature of the molecular environment around the tryptophan residue in this protein family.

Similary, the luminescent rare earth cation $Tb^{3+}$ has been used as an analogue of $Ca^{2+}$ (Richardson, 1985; Reuben, 1979). In such studies tryptophan often exhibits RET[1] to $Tb^{3+}$. We have exploited this effect to complement our studies on the relation between the environment of the tryptophan and the $Ca^{2+}$ site in p36 and p36–p11 complex.

## Materials and Methods

Ultrapure imidazole was purchased from Fluka Chemical Co. (Neu Ulm, FRG) and *p*-terphenyl from Lambda Physik (Göttingen, FRG). Deionized and Millipore-filtered water was used throughout this study. $Tb(ClO_4)_3$ stock solution was prepared from terbium oxide (99.999%) from Alfa (Karlsruhe, FRG). Tryptophan from Sigma (St. Louis, MO) was refluxed with activated charcoal and twice recrystallized from 5% ethanol for quantum yield comparisons, and NATA from Sigma was desiccated over silica gel and anhydrous calcium

† G.M. was supported by a fellowship from the Alexander von Humboldt Stiftung. W.R.K. and N.J. were supported by fellowships from the Max Planck Society.

* Authors to whom correspondence should be addressed.
‡ Department of Molecular Biology.
§ Present address: Department of Physics, Faculty of Science and Technology, Keio University, 14-1 Hiyoshi 3-Chome, Yokohama, Japan.
‖ Department of Biochemistry.

[1] Abbreviations: DMF, dimethylformamide; EGTA, ethylene glycol bis(β-aminoethyl ether)-*N*,*N*,*N*′,*N*′-tetraacetic acid; NATA, *N*-acetyltryptophanamide; RET, resonance energy transfer; THF, tetrahydrofuran.

0006-2960/90/0429-7004$02.50/0 

chloride under reduced pressure. DMF was purchased from Burdick and Jackson (Madison, WI) and used directly, and THF (Baker HPLC grade) was dried prior to use by passage over an activated alumina column (Woelm, Eschwege, FRG).

*Purification of Proteins.* Porcine, human, and chicken p36–p11 complexes were purified according to Gerke and Weber (1984) with minor modifications (Johnsson et al., 1988). Porcine p36 and p11 subunits were separated and renatured as previously described (Gerke & Weber, 1985). Protein pII was purified according to Shadle et al. (1985). All measurements except where noted were made at 20 °C in 20 mM imidazole hydrochloride, 100 mM sodium chloride, and 50 μM EGTA, pH 7.5, at protein concentrations between 5.0 and 10 μM. Calcium chloride was added to the $Ca^{2+}$-free buffer to a final concentration of 1 mM to ensure complete complexation of the protein.

*Instrumentation and Spectroscopy.* Absorption difference spectra were recorded on a Cary 118 spectrophotometer between 250 and 320 nm. Corrected, steady-state fluorescence excitation and emission spectra were recorded on an SLM Model 8000 spectrofluorometer (Urbana, IL). The Wood's anomalies inherent in the SLM excitation monochromator were removed by the introduction of a quartz depolarizer (Melles Griot), which was placed directly before the beam splitter of the SLM optical module (Marriott et al., 1988). The quantum counter rhodamine B was dissolved to a concentration of 10 mg/mL in methanol rather than ethylene glycol as is the normal practice, in order to minimize polarization of the emission reaching the phototube of the reference channel. Excitation and emission wavelengths for the stimulation and observation of the intrinsic protein and $Tb^{3+}$ emission are indicated in the figure legends. Background fluorescence and Raman scattering from the buffer were corrected in all sample spectra although these signals never exceeded 5% of the total protein fluorescence.

Quenching studies of the tryptophan emission in p36, and p36–p11 complex, as well as protein II were performed by adding aliquots of a 2 M potassium iodide solution containing 1 mM sodium thiosulfate to a 5 μM solution of the protein serially up to a final iodide ion concentration of 0.2 M; emission spectra were recorded between 300 and 450-nm (4-nm bandwidth) with an excitation wavelength of 295 nm (4-nm bandwidth), and the integrated fluorescence signals were corrected for dilution effects. Steady-state fluorescence excitation polarization spectra were recorded manually on the same fluorometer using an L-format configuration and employing corrections of the polarization response of the detection system. The value of the polarization of the fluorescence reported is the average of three separate determinations; the error in the averaged value was between 0.001 and 0.002 polarization unit. Fluorescence intensity decay measurements of the intrinsic emission of $Ca^{2+}$-free and -bound p36 were performed on a multifrequency phase and modulation fluorometer designed and built in the Department of Molecular Biology of this institute and in the Laboratory for Fluorescence Dynamics of the University of Illinois and described in detail by Piston et al. (1989). The proteins were excited with the full deep ultraviolet output (to 301 nm) of a c.w. Spectra physics 2035 argon ion laser, and the emission was collected through a 320- or 340-nm interference filter with a 10-nm band-pass (Corion Corp.). *p*-Terphenyl dissolved in cyclohexane was used as a reference fluorescence lifetime of 1 ns. The frequency response of the emission upon excitation with sinusoidally modulated light was determined at 20 or more frequencies spread logarithmically over 3 decades. Phase-delay data were analyzed by global analysis with the commercial software package Globals Unlimited (Laboratory for Fluorescence Dynamics, Urbana, IL).

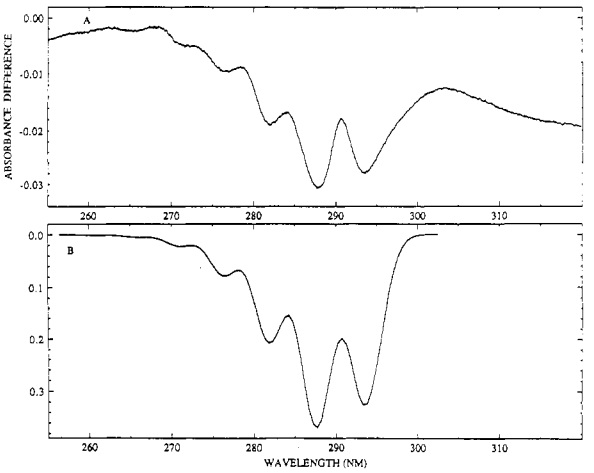


FIGURE 1: (Panel A) Absorption difference spectrum for p36 (26 mM, $E_{280} = 7.2 \times 10^4$ cm$^2$/mmol) without $Ca^{2+}$ subtracted from p36 with addition of 1 mM $Ca^{2+}$. (Panel B) Fit of spectrum A to Huang and Rhys (1950) Franck–Condon factors for a single harmonic oscillator with a frequency of 710 cm$^{-1}$, horizontal displacement of harmonic potential of 0.10 Å [1.5 times the oscillator expectation value of $(h/2\pi M\omega)^{1/2}$; see Siebrand, (1966)], and reduced mass of 10 amu. From the data we have surmised a Gaussian "broadening" of $e^{-(\nu-\nu_0)^2/\sigma^2}$ with $\sigma$ equivalent to 1.54 kT (Englman & Jortner, 1970).

## RESULTS

*Absorption Difference Spectrum of $Ca^{2+}$-Free and -Bound p36.* The ultraviolet absorption spectrum of $Ca^{2+}$-bound p36 is blue-shifted with respect to that of the free protein (data not shown). The ultraviolet absorption *difference* spectrum of $Ca^{2+}$-free and -bound p36 is shown in Figure 1A. Upon $Ca^{2+}$ binding there are a number of negative difference peaks distributed over the entire ultraviolet-absorbing region, which are unique to p36 and p36–p11 complex (Gerke & Weber, 1985). If we concentrate for the moment just on the difference envelope, it displays a center of mass close to 290 nm, suggesting major involvement of the tryptophan residue. The obvious structure within the envelope, however, exhibits a progression of approximately 710 cm$^{-1}$, which we have deconvoluted into a set of Gaussianly broadened Franck-Condon factors (Figure 1B)—representing the nuclear overlap between the ground and $^1L_a$ electronic states of tryptophan—for a single vibrational mode at this frequency (Huang & Rhys, 1950; Byrne et al., 1965; Siebrand, 1967; Englman & Jortner, 1970). It is interesting that the $^1L_a$ transition seems to be more sensitive to changes in its surroundings in general than the $^1L_b$ transition [cf. Lami and Glasser (1986)]. We thus expect that the $Ca^{2+}$ site must be close enough to the tryptophan to at least interact with its neighboring groups to bring about a vacancy in this vibrational mode. The explanation that the $Ca^{2+}$-dependent difference spectrum arises essentially from the sole tryptophan residue of p36 fits the observations that a proteolytic derivative of p36 covering residues 30–204, i.e., the first two repeat segments, displays no difference spectrum but nonetheless binds to acidic phospholipids in a $Ca^{2+}$-dependent manner [see Discussion and Johnsson and Weber (1990)].

*Steady-State Fluorescence Emission and Excitation Spectra of Porcine p36. (A) $Ca^{2+}$ Free.* The dependence of the intrinsic fluorescence emission spectrum of porcine $Ca^{2+}$-free p36 on the excitation wavelength is shown in Figure 2. The contribution to the total emission signal from the tryptophan residue is revealed by the increasing red-shift of the spectrum

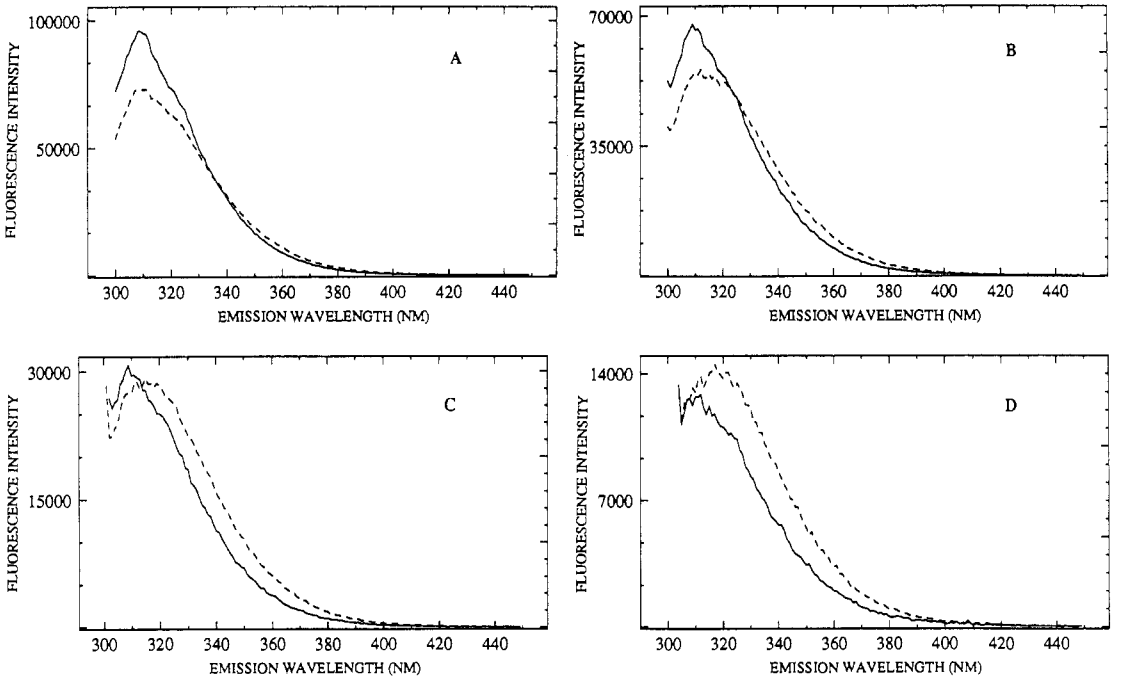


FIGURE 2: Corrected steady-state fluorescence emission spectra of a 5 $\mu$M solution of porcine p36 in $Ca^{2+}$-free (--) and 1 mM $Ca^{2+}$ (—) buffer as a function of the excitation wavelength: (panel A) 290 nm; (panel B) 295 nm; (panel C) 297 nm; (panel D) 299 nm. Excitation and emission bandwidths were set at 4 nm. Data were acquired at 1 s/nm.

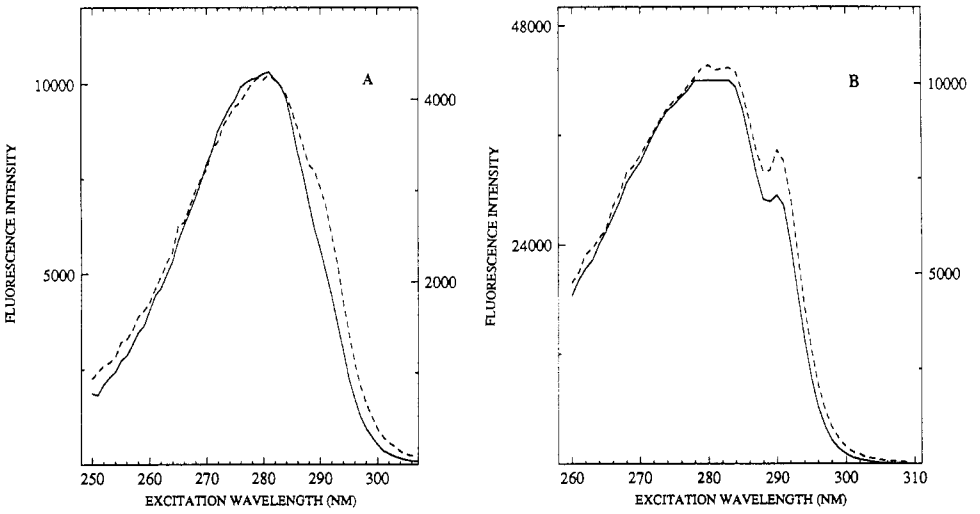


FIGURE 3: Normalized and corrected steady-state excitation spectra of a 5 $\mu$M solution of porcine p36 in (A) $Ca^{2+}$-free buffer and (B) 1 mM $Ca^{2+}$ buffer. Spectra were recorded at emission wavelengths of 315 (—) and 350 nm (--). Excitation and emission bandwidths were set at 4 nm.

upon excitation of the protein through wavelengths above 290 nm. With excitation above 295 nm the emission exhibits a maximum at about 320 nm. The normalized fluorescence excitation spectra of the 315- and 350-nm emissions of porcine p36 are shown in Figure 3A. Although the characteristic shoulder of the $^1L_a$ transition of tryptophan can be seen in both these spectra, it is resolved better at 350 nm.

*(B) In the Presence of $Ca^{2+}$.* The tryptophan emission spectrum of p36 is even further blue-shifted upon the addition of 1 mM $Ca^{2+}$ (Figure 2). This finding is particularly evident with excitation of the protein between 295 and 299 nm when the wavelength of maximum emission is shifted from 320 nm to approximately 312 nm. The progressive inversion of the steady-state fluorescence intensity ratio of the $Ca^{2+}$-free and -bound p36 emissions with excitation from 290 to 299 nm (Figure 2) results from the blue-shift in the absorption spectrum of p36 upon binding $Ca^{2+}$. The fluorescence excitation spectra of $Ca^{2+}$-bound porcine p36 at 315 and 350 nm are shown in Figure 3B. There is a noticeable blue-shift in this excitation when compared with that of the free p36, corresponding to what is observed in absorption. The characteristic shoulder of the indole $^1L_a$ transition centered at 290 nm is very well resolved in both these spectra, in contrast to the corresponding spectra of $Ca^{2+}$-free p36 (Figure 3A); this effect is a consequence of the $Ca^{2+}$-induced blue-shift in the tryptophan excitation spectrum. The buried nature of the tryptophan residue in $Ca^{2+}$-free p36 and $Ca^{2+}$-bound p36 was confirmed on the basis of observations that iodide ions up to a final concentration of 0.2 M did not quench the tryptopan fluorescence (data not shown).

*Excitation Polarization Spectra of Porcine p36.* We expanded our investigations into the nature of the red-edge excitation properties of p36 and $Ca^{2+}$–p36 by examining their excitation polarization spectra. The spectrum of the $Ca^{2+}$-bound p36 is blue-shifted with respect to that of the $Ca^{2+}$-free p36 (Figure 4), consistent with our findings in the absorption

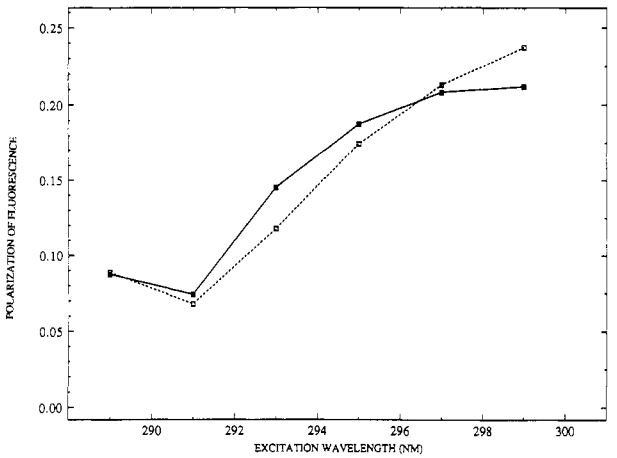


FIGURE 4: Steady-state excitation polarization spectra of a 5 $\mu$M solution of porcine p36 in $Ca^{2+}$-free (--) and 1 mM $Ca^{2+}$ (—) buffer. Spectra were recorded at an emission wavelength of 315 nm. Excitation and emission bandwidths were set at 2 and 4 nm, respectively.

difference spectrum (Figure 1A) and the excitation spectra (Figure 3). This arises, presumably, from the large spectral overlap between $^1L_b$ and $^1L_a$ transitions, which in many solvents does not attenuate until roughly 305 nm (Weber, 1960; Valeur & Weber, 1977). That the polarization of $Ca^{2+}$–p36 emission already attains a plateau value by 297 nm suggests that in this protein we excite effectively a purely $^1L_a$ transition in this region. For the $Ca^{2+}$-free protein, even with some remaining contribution from $^1L_b$ in this spectral region (as suggested by the steady increase in the polarization), the value of the polarization is significantly higher. This could be due to either (a) an increase in the rotational freedom of the tryptophan upon $Ca^{2+}$ binding or (b) an increased fluorescence lifetime of the tryptophan with $Ca^{2+}$ bound. Our results (see Fluorescence Lifetime Measurements) suggest that the latter is a sufficient explanation, since the average lifetime of the 320-nm emission in the presence of $Ca^{2+}$ is 2.1 ns and in its absence 1.5 ns.

*Binding of $Tb^{3+}$ to Porcine p36.* $Tb^{3+}$ binds to p36 and exhibits a sensitized emission at 488 and 544 nm upon excitation of the protein at 290 nm (Figure 5A). Interestingly, $Tb^{3+}$ does not elicit a change in the environment of the single tryptophan residue to the same extent as $Ca^{2+}$ as monitored by its intrinsic emission since the spectrum of $Tb^{3+}$-bound p36 is blue-shifted to a lesser degree than that found for $Ca^{2+}$-bound p36 (in Figure 2). We have used the emission of $Tb^{3+}$ in the presence and absence of p36 to investigate the identity of the RET donor in p36. The excitation spectrum of the terbium ion's 544-nm emission corresponds to that found for tryptophan alone (Figure 5B). Since $Ca^{2+}$ is saturating at millimolar concentrations (Gerke & Weber, 1985), we assumed that $Tb^{3+}$ binding is also saturated at the concentration employed. We can calculate the efficiency of transfer from comparison of the emission of p36 excited at 295 nm with the resultant $Tb^{3+}$ emission. The efficiency of transfer $E_{Tr}$ is related to the emission ratio by

$$E_{Tr}\Phi_{Tb}/(\Phi_{320}f_{320} + \Phi_{340}f_{340}) = I_{Tb}/I_{prot}$$

where the $I$'s are the emission intensities, $\Phi$'s are the quantum yields, and $f$'s are the fractional intensities of the "short"- and "long"-wavelength components obtained from the emission spectrum; i.e., the summed emission intensity from 300 to 330 nm and that from 330 to 400 nm are normalized to 1.00, with values of 0.39 and 0.61, respectively. These regions are treated separately because we obtain different lifetime/fractional intensity ratios at these wavelengths (see Table I), yet there is no spectroscopic or other evidence of heterogeneity in the sample. We ascribe this difference instead to intrinsic variation of the emission dipole characteristics (see Discussion). Assuming, therefore, a distinction in the quantum yield of the emission at 320 and 340 nm, we obtain distinct values for $k_{Tr,i}$, the transfer rate in each of the two emission regions. These in turn are summed to give the total $k_{Tr}$ expected at a given separation of the donor and acceptor dipoles, $R_{Tb-Trp}$. In this way, calculating the energy transfer probability with the known extinction of $Tb^{3+}$ bands [from the analytic formula given by Kirk and Amzel (1987)], we find the largest transfer channel is to the 341-nm $Tb^{3+}$ band. Employing, in the usual Foerster (1964) expression for $k_{Tr,i}$

$$k_{Tr,i} = (R_{o,i}^6/R_{Tb-Trp}^6)/\langle\tau_i\rangle = (8.789 \times 10^{-25})\langle\kappa^2\rangle(\Phi_{donor}/R_{Tb-Trp}^6 n^4\langle\tau\rangle)\int f(\lambda)\epsilon(\lambda)\lambda^4\, d\lambda$$

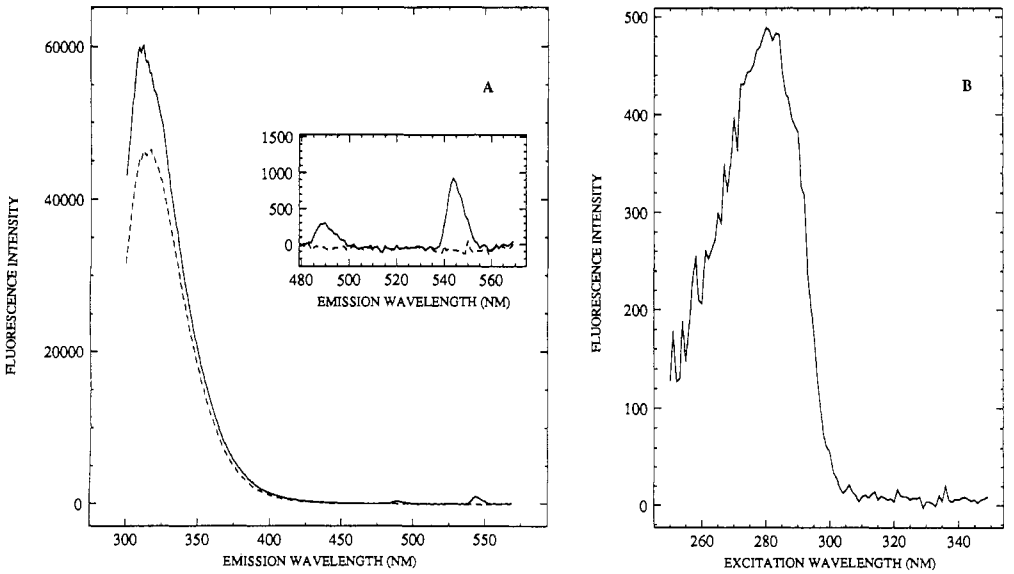


FIGURE 5: (A) Corrected steady-state emission spectra of porcine p36 in $Ca^{2+}$-free (--) and 1.29 mM $Tb^{3+}$ (—) buffer with excitation of the sample at 290 nm. The $Tb^{3+}$-bound p36 spectrum was corrected for the emission of unbound $Tb^{3+}$. Excitation and emission bandwidths were set at 4 and 2 nm, respectively. (B) Corrected steady-state ultraviolet excitation spectrum of $Tb^{3+}$-bound procine p36 collected at the 545-nm $Tb^{3+}$ emission. The spectrum was corrected for the contribution from unbound $Tb^{3+}$. Excitation and emission bandwidths were set at 1 and 8 nm, respectively. Data were acquired at a rate of 10 s/nm.

Table I: Comparisons of Fluorescence Quantum Yields and Lifetimes

| | $\alpha_1$ | $\tau_1$ | $\alpha_2$ | $\tau_2$ | $\Phi$ | "$\chi^{2}$" [a] |
|---|---|---|---|---|---|---|
| tryptophan in $H_2O$ [b] | 0.82 | 3.26 | 0.18 | 0.80 | 0.119 | |
| NATA [c] in DMF (emission max 333 nm) | 1.00 | 4.00 | | | 0.15 [d] | |
| NATA in THF (emission max 324 nm) | 0.60 | 4.03 | 0.40 | 0.23 | 0.19 [e] | 2.75 |
| tryptophan in p36 | | | | | | |
| +$Ca^{2+}$ | | | | | | |
| 340-nm emission | 0.313 | 3.32 | 0.687 | 1.14 | | 1.87 |
| 320-nm emission | 0.214 | 4.54 | 0.787 | 1.44 | | 2.35 |
| +EGTA | | | | | | |
| 340-nm emission | 0.141 | 4.85 | 0.859 | 1.32 | 0.08 [f] | 0.38 |
| 320-nm emission | 0.121 | 4.24 | 0.879 | 1.14 | 0.12 [g] | 0.65 |

[a] $\alpha_i$ gives the amplitude of the $i$th decay component of lifetime $\tau_i$, "$\chi^{2}$" gives the chi-square value from the fitting routine of Globals Unlimited, which does not account for variance at each frequency, $\Phi$ gives the quantum yield of total or partial emission. [b] Data from Ross and Brand (1983); quantum yield from Borreson (1967). [c] *N*-Acetyltryptophanamide. Parameters determined by the authors with 295-nm excitation and 320-nm emission monitored, except where noted. [d] By direct comparison of emission intensity against tryptophan, with refractive index corrections included [see Demas and Crosby (1971)]. [e] As in footnote *d*. However, the calculated $k_{rad}$ for this system is $8 \times 10^7$/s vs. $4.2 \times 10^7$/s for tryptophan and NATA; see footnotes *f* and *g* below. [f] From a $k_{rad}$ of $4.2 \times 10^7$/s and an effective lifetime equal to $\langle\tau\rangle = \sum\alpha_i\tau_i$. [g] From a $k_{rad}$ of $8.0 \times 10^7$/s, similar to that obtained from NATA in THF and tryptophan in apoazurin (Hutnik & Szabo, 1989); $\langle\tau\rangle$ as defined in footnote *f*.

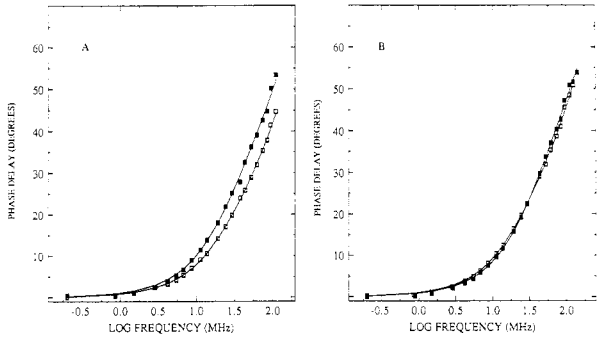


FIGURE 6: Multifrequency phase delay data and fit for the decay of the intrinsic fluorescence intensity of a 10 $\mu$M solution of porcine p36 collected at (A) 320 and (B) 340 nm in $Ca^{2+}$-free (open squares) and 1 mM $Ca^{2+}$ (closed squares) buffer.

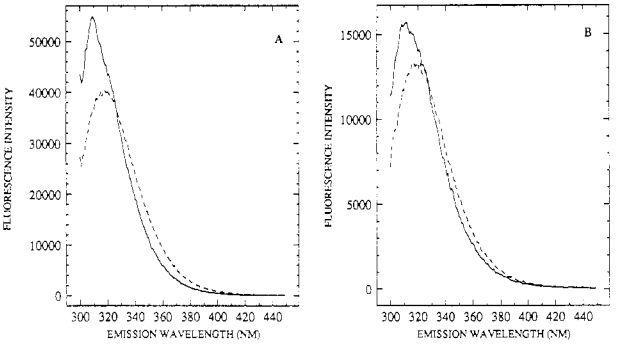


FIGURE 7: (A) Corrected steady-state emission spectra of human and chicken p36 in the presence and absence of $Ca^{2+}$ upon excitation at 295 nm. Excitation and emission bandwidths were set at 4 nm. (B) Corrected steady-state emission spectra of porcine p36–p11 complex in the presence and absence of $Ca^{2+}$ upon excitation at 295 nm. Excitation and emission bandwidths were set at 4 nm.

the nominal index of refraction raised to the fourth power representing a squared screening constant on the product of donor and acceptor oscillator strengths, we obtain an $R_0$ of 3.4 ± 0.4 Å. In the above expression, the terms have their usual meaning; i.e., $\epsilon(\lambda)$ is the molar decadic extinction coefficient as a function of wavelength, and the values for $\langle\tau_i\rangle$ are given as described in Table I and footnote *f* to the table.

Since the $Tb^{3+}$ emission represents 0.5% of the protein emission and given that the quantum yield of $Tb^{3+}$ is most likely to be between 0.03 and 0.12 (Dawson et al., 1966), on the basis of the existence of a large deuterium solvent isotope effect on its emission (data not shown), we can calculate a distance of roughly 7.8 ± 1.7 Å between the effective dipoles of tryptophan and $Tb^{3+}$ in p36. The uncertainties on these values do not reflect statistical standard deviations but rather the total allowed distribution in the values of $\langle\kappa^2\rangle$ for an isotropic acceptor like $Tb^{3+}$ [see Dale and Eisinger (1974)] and the range of values for its quantum yield.

*Fluorescence Lifetime Measurements.* We have fit using two exponentials the phase-delay data for tryptophan in p36 and $Ca^{2+}$-bound p36 in a variety of model systems (Table I and Figure 6; analysis of these data using three exponentials did not improve the quality of the fit, nor did they suggest the presence of a significant Raman scattering signal). While we make no claim that this represents an exhaustive study of tryptophan emission in general, we can obtain a better perspective of the relationships in p36 between the lifetimes we obtained at differing emission wavelengths and in the presence vs the absence of $Ca^{2+}$ by our further comparisons of quantum yield and lifetimes employing these model solvent systems with the peptide tryptophan analogue *N*-acetyltryptophanamide, as well as with certain values from the literature.

*Summary of Intrinsic Fluorescence Emission Properties of Human and Chicken p36, Porcine p36–p11 Complex, and Porcine pII.* We have found that $Ca^{2+}$-free and $Ca^{2+}$-bound human p36 and chicken p36 (data not shown) and the porcine p36–p11 complex exhibit emission properties similar to those of porcine $Ca^{2+}$-free and -bound p36 (Figure 7). The similarity in the blue-shifted emission spectra of $Ca^{2+}$-bound p36 and heterotetrameric p36–p11 complex suggests that the tryptophan residue is not located at the p11–p36 interface in the complex. The dependence of the fluorescence emission spectra of $Ca^{2+}$-free protein II on the excitation wavelength (Figure 8A) is similar to that observed for $Ca^{2+}$-free p36 (Figure 2). On the basis of absorption difference measurements (Shadle et al., 1985), protein II is known to bind $Ca^{2+}$. However, the tryptophan emission properties are only slightly modified upon formation of the $Ca^{2+}$–protein II complex (Figure 8B). This contrast in the sensitivity of the p36 and protein II tryptophan emissions to $Ca^{2+}$ binding probably reflects the difference in the molecular environment of this residue within these proteins; the tryptophan residue of protein II is shifted only seven amino acids to the N-terminus with respect to that of p36. This observation highlights the fact that the emission properties of fluorophores are very sensitive to modifications of their interactions and dynamics only in their immediate environment (Weber, 1983). The tryptophan residue of $Ca^{2+}$-free and -bound protein II is not exposed to solvent molecules since iodide ions up to a concentration of 0.2 M do not modify the emission (data not shown).

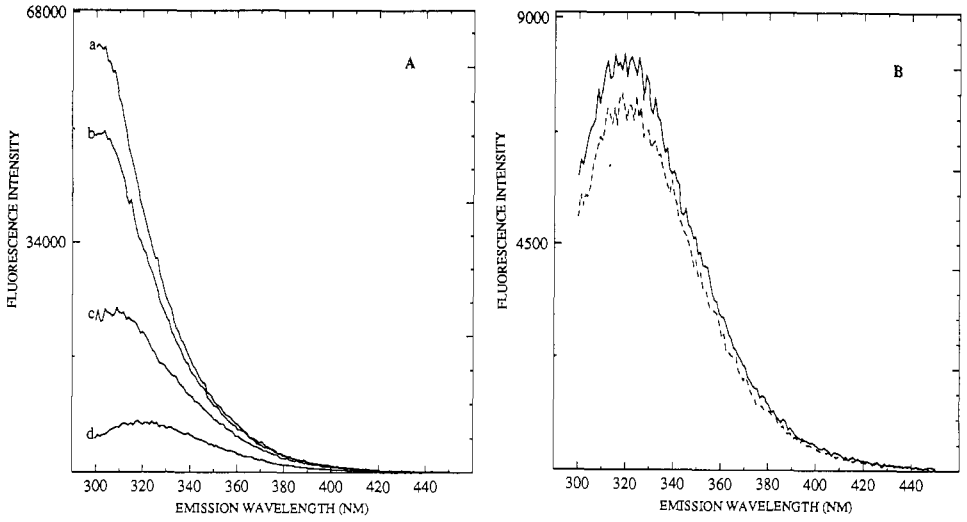


FIGURE 8: (A) Dependence of the corrected steady-state emission spectrum of $Ca^{2+}$-free porcine protein II on the excitation wavelength. The protein was excited at (a) 280, (b) 285, (c) 290, and (d) 295 nm. Excitation and emission bandwidths were set at 4 nm. (B) Corrected steady-state emission spectra of porcine protein II in $Ca^{2+}$-free (--) and 1 mM $Ca^{2+}$ (—) buffer. Excitation wavelength was 295 nm. Excitation and emission bandwidths were set at 4 nm.

## Discussion

*Intrinsic Fluorescence Emission of p36 and the p36–p11 Complex in the Presence and Absence of $Ca^{2+}$ Obeys Teale's Rule.* In class B proteins, i.e., those containg both tyrosine and tryptophan residues, the fluorescence emission observed with excitation at 295 nm or longer originates, according to Teale's (1960) rule, from the tryptophan residue. Recently, however, Willis and Szabo (1989) have shown that the emission of at least one single-tryptophan protein does not obey Teale's rule. Specifically, these authors studied steady-state and time-resolved emission properties of the enzyme subtilisin Carlsberg and found that a tyrosine emission component accounted for approximately 49% of the total protein fluorescence signal upon excitation at 295 nm and contributed 25% to the total emission with 305-nm excitation. In light of this report, we sought to confirm the adherence of the intrinsic fluorescence emissions of $Ca^{2+}$-free and -bound p36, and p36–p11 complex, and protein II to Teale's rule. We summarize below the spectroscopic evidence we obtained which, we argue, makes this confirmation possible with these proteins. First, the emission spectra of all the proteins studied red-shift with increasing excitation wavelength. This effect is characteristic of class B proteins and is generally regarded as sufficient proof that tryptophan residues are present in a protein (Teale, 1960). Second, the fluorescence excitation spectra of $Ca^{2+}$-free and -bound p36 display the characteristic $^1L_a$ band of indole when observed at the maximum and on the red side of the emission spectrum (Figure 3); if the emission from the tyrosine residues dominated the fluorescence signal in these regions, then the characteristic spectral excitation profile of $^1L_a$ from the indole would be largely submerged in the tyrosine signal. Third, the excitation polarization spectra of $Ca^{2+}$-free and -bound p36 bear the characteristic signature of a $^1L_a$ indole transition (Figure 4), which is clearly distinguishable in both energy and shape from the excitation polarization spectral profile of tyrosine (Weber, 1960). Finally, we know that the blue-shifted emission spectrum of $Ca^{2+}$-bound p36 does not result from the excitation of tyrosine residues with an unusually red-shifted ground state, since $Ca^{2+}$ binding induces a *blue*-shift only in the tryptophan absorption regime (Figure 1A).

*Spectroscopic Effects of Hydrogen Bonding of the Imino Proton of Tryptophan in Model Solvents: An Interpretation of the Absorption and Fluorescence Spectroscopic Properties of Tryptophan in $Ca^{2+}$-Free and -Bound p36.* It is known that the spectroscopic properties of the ground and excited states of tryptophan are highly dependent on the state of hydrogen bonding of the imino proton (Konev, 1967; Demchenko, 1986). In particular, Strickland et al. (1970, 1972) and Cherkasov (1960) have shown that indole and a number of its derivatives dissolved in low-dielectric, non-hydrogen-bonding solvents may form specific hydrogen bonds upon the addition of small amounts of certain hydrogen-bond acceptor solvents such as DMF. In these studies the bulk physical properties of the apolar solvent such as the refractive index and the dielectric constant remain unchanged, yet specific cosolvent–fluorophore interactions result in red-shifts of the $^1L_a$ indole absorption and emission spectra of up to 9 and 30 nm, respectively. The combined peptide dipole content of any protein accounts for approximately 30% of the total volume. On the basis of dense packing within the protein matrix (Richardson, 1981), we would expect that specific dipolar or hydrogen-bond interactions between the carbonyl moiety of a peptide bond and the imino proton of tryptophan, for example, would be nearly unavoidable. This prediction is consistent with an analysis of the interaction of an extrinsic fluorophore within a protein matrix monitored by excitation spectral shifts and fluorescence Stokes shifts (Macgregor & Weber, 1986), as well as with the findings of a statistical analysis of the frequency and nature of hydrogen-bonding interactions within proteins (Baker & Hubbard, 1984).

We have separately treated the two spectral regions, 320 and 340 nm, because our lifetime data forces us to conclude that the quantum yield of the emission is not constant from 310 to 350 nm. This indicates that the tryptophan emission dipole is subject to some variation, whether induced by vibrations coupled to the protein matrix, fluctuations in hydrogen-bonding interactions, or different rotamers of the tryptophan itself, which gives it alternative radiative and possibly also nonradiative pathways. These difference are apparent in the $Ca^{2+}$-free protein, but they certainly persist, though are slightly diminished, in the $Ca^{2+}$-bound case.

On the basis of the characteristics of polar interactions within the protein matrix, we argue that the unusual absorption and emission characteristics of tryptophan in p36 upon binding $Ca^{2+}$ may arise from changes in the specific solvation of the

indole imino proton with a peptide dipole. We have found that the $Ca^{2+}$-free p36 excitation and emission spectra resemble those observed for tryptophan residues known to be buried and hydrogen bonded within the protein matrix, e.g., RNase T1 (Longworth, 1968), as well as that of indole dissolved in apolar solvents containing small amounts of polar, strong hydrogen-bond acceptor solvents such as DMF (Strickland et al., 1970). Upon formation of the p36–$Ca^{2+}$ complex, we believe a specific solvation, in the foregoing sense, of the imino proton with the polar peptide group may be broken or weakened, resulting in blue-shifted excitation and emission spectra similar to those found for indole in apolar, low-dielectric, non-hydrogen-bonding solvents (Meech et al., 1983). For comparison, the tryptophan residue of azurin from *Pseudomonas aeruginosa*, which inhabits a highly apolar environment within the protein matrix (Burstein et al., 1977; Petrich et al., 1987), displays excitation and emission spectra not too dissimilar from what we observe with p36. In this protein the single tryptophan occupies an environment devoid of peptide dipoles and other polar groups to within a radius of 5.2 Å of the imino proton.

The large blue-shift of the tryptophan emission spectrum of p36 upon $Ca^{2+}$ binding provides us with an indicator of how certain proteins may fine-tune the polarity of certain regions within their matrix. the functional relevance of this effect in the p36 family of proteins is unknown, although this phenomenon may be useful in those enzymes that require rapid modulations of the local polarizability and rotational or librational dynamics of the active site during catalytic steps.

*Implications for the Structure of the Annexins.* Tryptophan is a very rare residue in the core domain of the annexins, which are known to harbor the $Ca^{2+}$/lipid binding site(s) and are built from repetitive segments. Most but not all annexins have a single tryptophan in the core, which is situated in annexin repeat 3. In all cases except for p36 this tryptophan occupies the same relative position as in protein II. It lies directly at the N-terminal border of a high-homology sequence of 14 residues. This motif is typical for all annexin repeats, and it has been speculated that it is directly involved in $Ca^{2+}$ and/or $Ca^{2+}$–lipid binding (Geisow et al., 1986). Since chicken p36 displays virtually identical emission characteristics as p36 from human and pig, we predict that it has its single tryptophan in the same position as in the mammalian proteins. p36 is the only annexin so far known where the tryptophan lies in the middle of the motif sequence. The pronounced $Ca^{2+}$-dependent ultraviolet difference spectrum of p36 was originally used to document that p36 is a $Ca^{2+}$ binding protein (Gerke & Weber, 1984, 1985). We have now shown that this spectrum is fully accounted for by the unique tryptophan of p36 and found that the separation of the emission dipole of tryptophan and the $Ca^{2+}$ analogue $Tb^{3+}$ is about 8 Å. This strongly implicates the third annexin motif of p36 as a component of some $Ca^{2+}$ binding site. Since we have previously shown by limited proteolysis experiments that interaction between the repeat segments is a prerequisite for affine $Ca^{2+}$-promoted lipid binding in the intact protein, we cannot exclude the possibility that the tryptophan may sense $Ca^{2+}$ binding in an adjacent annexin repeat. Those p36 fragments that harbor either annexin repeat 1 or repeats 1 and 2 display only moderate $Ca^{2+}$ binding when assayed by $Ca^{2+}$-dependent lipid binding (Johnsson & Weber, 1990). The combined results indicate that, at least in p36, annexin repeats 1 and 3 harbor a $Ca^{2+}$ site. Such a conclusion fits, in general terms, reports on the number of $Ca^{2+}$/lipid binding sites for several annexins. For annexins with four segments these values range from two to four [for review, see Klee (1988)]. The motif sequence of segment 3, which we have now demonstrated to be involved in a $Ca^{2+}$ binding site, is being studied further with suitably modified annexins to ascertain whether the corresponding motifs in the other segments are also involved in additional $Ca^{2+}$ sites, as is already implicated for segment 1 of p36. It also remains to be seen whether the $Ca^{2+}$-induced lipid binding involves the same motif or an additional sequence. In spite of these reservations, the molecular identification of the motif involved in $Ca^{2+}$ binding can now be used in various ways to identify the ligands on the $Ca^{2+}$ binding site.

## Acknowledgments

We thank Dr. Thomas M. Jovin for use of instrumentation and facilities within his department and Dr. Robert Clegg for helpful discussions.

## References

Baker, E. N., & Hubbard, R. E. (1984) *Prog. Biophys. Mol. Biol.* 44, 97–197.

Beechem, J., & Brand, L. (1986) *Photochem. Photobiol. 44* (3), 323–329.

Børreson, H. C. (1967) *Acta Chem. Scand. 21*, 920–936.

Burstein, E. A., Permyakov, E. A., Yashin, V. A., Burklanov, S. A., & Finazzi-Agro, A. (1977) *Biochim. Biophys. Acta 491*, 155–163.

Byrne, J. P., McCoy, E. F., & Ross, I. G. (1965) *Aust. J. Chem. 15*, 573–582.

Cherkasov, A. S. (1960) *Akad. Nauk SSSR, Bull. Phys. Sci. 24*, 597–601.

Dale, R. E., & Eisinger, J. (1974) *Biopolymers 13*, 1573–1605.

Dawson, W. R., Kropp, J. C., & Windsor, M. W. (1966) *J. Chem., Phys. 45*, 2410–2418.

Demas, J. N., & Crosby, G. A. (1971) *J. Phys. Chem. 75* (8), 991–1024.

Demchenko, A. P. (1986) in *Ultraviolet Spectroscopy of Proteins*, pp 34–40, 64–90, Springer-Verlag, Berlin.

Englman, R., & Jortner, J. (1970) *Mol. Phys. 18*, 145–163.

Foerster, T. (1964) *Modern Quantum Chemistry* (Sinanoglu, O., Ed.) pp 93–137, Academic Press, New York.

Geisow, M. J., Fritsche, U., Hexham, J. M., Dash, B., & Johnson, T. (1986) *Nature (London) 320*, 636–638.

Gerke, V., & Weber, K. (1984) *EMBO J. 3*, 227–233.

Gerke, V., & Weber, K. (1985) *J. Biol. Chem. 260*, 1688–1695.

Glenney, J. R. (1986) *J. Biol. Chem. 201*, 7247–7252.

Huang, K., & Rhys, A. (1950) *Proc. R. Soc. London, A 204*, 406–411.

Hutnik, C. M., & Szabo, A. (1989) *Biochemistry 28*, 3923–3934.

Johnsson, N., & Weber, K. (1990) *Eur. J. Biochem. 188*, 1–7.

Johnsson, N., Vandekerckhove, J., van Damme, J., & Weber, K. (1986a) *FEBS Lett. 198*, 361–364.

Johnsson, N., Van, P. N., Söling, M. D., & Weber, K. (1986b) *EMBO J. 5*, 3455–3460.

Johnsson, N., Marriott, G., & Weber, K. (1988) *EMBO J. 7*, 2435–2442.

Kirk, W. R., & Amzel, L. M. (1987) *Biochim. Biophys. Acta 916*, 304–312.

Klee, C. (1988) *Biochemistry 27*, 6645–6653.

Konev, S. V. (1967) in *Fluorescence and Phosphorescence of Proteins and Nucleic Acids*, Plenum Press, New York

Lakowicz, J. R., & Weber, G. (1973) *Biochemistry 12*, 4171–4179.

Lami, H., & Glasser, N. (1986) *J. Chem. Phys. 84* (2), 597–604.

Longworth, J. W. (1968) *Photochem. Photobiol. 7*, 587–595.

Longworth, J. W. (1986) in *Time Resolved Fluorescence Spectroscopy in Biochemistry and Biology*, Proceedings of a NATO Advanced Study Institute, St. Andrews (Cundall, R. B., & Dale, R. E., Eds.) pp 651–725, Plenum Press, New York.
Macgregor, R. B., Jr., & Weber, G. (1986) *Nature (London) 318*, 70–73.
Marriott, G., Zechel, K., & Jovin, T. M. (1988) *Biochemistry 27*, 6214–6220.
Meech, S. R., Phillips, D., & Lee, A. G. (1986) *Chem. Phys. 80*, 317–328.
Petrich, J. W., Longworth, J. W., & Fleming, G. R. (1987) *Biochemistry 26*, 2711–2722.
Piston, D., Marriott, G., Clegg, R. M., Radivoyevitch, T., Jovin, T. M., & Gratton, E. (1989) *Rev. Sci. Instrum. 60*, 2596–2600.
Reuben, J. (1979) in *Handbook on the Physics and Chemistry of Rare Earths* (Gschneider, K. A., & Eyring, L., Eds.) pp 515–552, North-Holland Amsterdam.
Richardson, F. (1982) *Chem. Rev. 82*, 541–552.
Richardson, J. S. (1981) *Adv. Protein Chem. 34*, 167–191.
Ross, J. B. A., & Brand, L. (1986) in *Time Resolved Fluorescence Spectroscopy in Biochemistry and Biology*, Proceedings of a NATO Advanced Study Institute, St. Andrews (Cundall, R. B., & Dale, R. E., Eds.) pp 635–643, Plenum Press, New York.
Saris, C. J. M., Tack, B. F., Kristensen, T., Glenney, J. R., & Hunter, T. (1986) *Cell 46*, 201–212.
Scarlata, S., Rholam, R., & Weber, G. (1984) *Biochemistry 23*, 6789–6792.
Shadle, P., Gerke, V., & Weber, K. (1985) *J. Biol. Chem. 260*, 16354–16360.
Siebrand, W. (1966) *J. Chem. Phys. 44*, 4055–4064.
Strickland, E. H., Horwitz, J., & Billups, C. (1970) *Biochemistry 9*, 4914–4921.
Strickland, E. H., Billups, C., & Kay, E. (1972) *Biochemistry 11*, 3657–3662.
Teale, F. W. J. (1960) *Biochem. J. 76*, 381–388.
Valeur, B., & Weber, G. (1977) *Photochem. Photobiol. 25*, 441–444.
Weber, G. (1960) *Biochem. J. 75*, 335–345.
Weber, G. (1983) in *Time Resolved Fluorescence Spectroscopy in Biochemistry and Biology*, Proceedings of a NATO Advanced Study Institute, St. Andrews (Cundall, R. B., & Dale, R. E., Eds.) pp 1–20, Plenum Press, New York.
Weber, K., Johnsson, N., Plessman, U., Van, P. N., Söling, H. D., Ampe, C., & Vandekerckhove, J. (1987) *EMBO J. 6*, 1599–1604.
Willis, K. J., & Szabo, A. G. (1989) *Biochemistry 28*, 4902–4908.
Xu, G.-J., & Weber, G. (1982) *Proc. Natl. Acad. Sci. U.S.A. 79*, 5268–5271.

# Folding and Stability of *trp* Aporepressor from *Escherichia coli*†

Mitchell S. Gittelman‡ and C. Robert Matthews*
*Department of Chemistry, The Pennsylvania State University, University Park, Pennsylvania 16802*
*Received November 30, 1989; Revised Manuscript Received April 4, 1990*

ABSTRACT: Equilibrium and kinetic studies of the urea-induced unfolding of *trp* aporepressor from *Escherichia coli* were performed to probe the folding mechanism of this intertwined, dimeric protein. The equilibrium unfolding transitions at pH 7.6 and 25 °C monitored by difference absorbance, fluorescence, and circular dichroism spectroscopy are coincident within experimental error. All three transitions are well described by a two-state model involving the native dimer and the unfolded monomer; the free energy of folding in the absence of denaturant and under standard-state conditions is estimated to be 23.3 ± 0.9 kcal/mol of dimer. The midpoint of the equilibrium unfolding transition increases with increasing protein concentration in the manner expected from the law of mass action for the two-state model. We find no evidence for stable folding intermediates. Kinetic studies reveal that unfolding is governed by a single first-order reaction whose relaxation time decreases exponentially with increasing urea concentration and also decreases with increasing protein concentration in the transition zone. Refolding involves at least three phases that depend on both the protein concentration and the final urea concentration in a complex manner. The relaxation time of the slowest of these refolding phases is identical with that for the single phase in unfolding in the transition zone, consistent with the results expected for a reaction that is kinetically reversible. The two faster refolding phases are presumed to arise from slow isomerization reactions in the unfolded form and reflect parallel folding channels.

The great majority of the studies on protein folding have focused on small monomeric globular proteins [for reviews, see Goldenberg (1988), Jaenicke (1987), Creighton (1984), and Kim and Baldwin (1982)]. The high degree of reversibility and the unimolecular folding kinetics have made this class of proteins an attractive target. Although these efforts have the potential to provide information on how the amino acid sequence determines the secondary and tertiary structure, issues on quaternary structure cannot be addressed.

To answer such questions, Jaenicke and others have examined the folding mechanism of a number of dimeric and tetrameric enzymes [see Jaenicke (1987) for a review]. For

†This work was supported by the National Institute of General Medical Sciences, Grant GM23303, and the National Science Foundation, Grant DMB-8705673.
‡Present address: Department of Molecular Biophysics and Biochemistry, Yale University, New Haven, CT 06510.

0006-2960/90/0429-7011$02.50/0 